E JOURNAL

Scanpath Centric Design for miniaturizing PBF-LB/M Prints

Ir Rein van der Mast [a,c], Ing Bert Hoekzema [b], Prof Dr Ir Brecht Van Hooreweder [c]

[a] Dept. of Mechanical Engineering, Fontys, BIC 1, 5657 BX Eindhoven, The Netherlands

[b] FMI Instrumed, De Brauwweg 17, 3125 AE Schiedam, The Netherlands

[c] Dept. of Mechanical Engineering, KU Leuven, Celestijnenlaan 300, 3001 Heverlee, Belgium.

https://doi.org/10.58134/fh-aachen-rte_2024_012

Zusammenfassung Die Pulverbettfusion mit Laserstrahl von Metallen (PBF-LB/M) ermöglicht die Übertragung fester Modelle („solids") und nichtfester Modelle („surfaces") in den physikalischen Bereich, z.B. materialisiert werden. Typischerweise werden Volumenkörper zur Darstellung von Teilen verwendet, und sowohl Volumenkörper als auch Nichtkörper werden als Stützstrukturen verwendet. Das weit verbreitete Konzept, ergänzt durch Konvertierungen namens „Slicing" und „Hatching", reicht in den meisten Fällen aus. Allerdings bleibt dem Ingenieur nur wenig Spielraum, die genaue Position des Scanpfads in jeder der Schichten zu steuern. Darüber hinaus erhält der Ingenieur im Produktdesignprozess, der die Materialisierung vornimmt, kein vollständiges Feedback über den Scanpfad. Die Studie versucht, einen Weg zu finden, diesen Mangel an Kontrolle zu überwinden, insbesondere bei kleinsten räumlichen Elementen, und zielt darauf ab, die Einsatzfähigkeit der Pulverbettschmelzung mit Laserstrahlen von Metallen in ihrer gängigsten Form zu erhöhen, einschließlich verbesserter Detaillierung. Es wurde eine neue Methode entwickelt, um Kurven zu erzeugen, die als Scanpfad fungieren und für den Ingenieur vollständig zugänglich sind. Beispiele für relevante Anwendungen dieser neuen Strategie sind (kleine, monolithisch integrierte) Blattfedern und Rohre, die durch die Anwendung dieses Ansatzes dichter, weniger rau und präziser und folglich weniger porös und haltbarer werden können.

Abstract Powder bed fusion with laser beam of metals (PBF-LB/M) allows for solid models ('solids') and non-solid models ('surfaces') to be transferred into the physical domain, e.g. to be materialized. Typically, solids are used to represent parts, and both solids and non-solids are used to act as support structures. The widely implemented concept, supplemented with conversions known as 'slicing' and 'hatching', is sufficient in most cases. However, it leaves only little room for the engineer to control the exact location of the scanpath in each of the layers. Furthermore, it does not provide full feedback about the scanpath to the engineer in the product design process proceeding the materialization. The study attempts to find a way to overcome such lack of control, particularly in case of the tiniest spatial elements, and aims to increase the deployability of powder bed fusion with laser beam of metals in its most popular form, including improved detailing. A new methodology was developed to generate curves to act as scanpath, fully accessible to the engineer. Examples of relevant applications for this new strategy include (small, monolithic integrated) leaf springs and tubes which by applying this approach may become denser, less rough and more accurate, and consequently less porous and more durable.

Introduction and motivation

Among several additive manufacturing (AM) processes, powder bed fusion with laser beam of metals (PBF-LB/M) stands out as a leading technology [1]. Most applications tend towards larger build volumes (500 × 500 × 500 mm^3 and more) and an increasing number of lasers (12 and rising) per chamber for higher productivity rates (over 1 dm^3/h) [2]. It can be said that they lack focus on the production of compact parts in which various functional elements are monolithically combined.

This study is based on the researchers' expectation, in contrast to the current trend, that the technology provides more opportunities for miniaturization than is known today, with potential for high-tech companies in realizing compact, complex systems, as well as companies that focus on small, personalized consumer products, like hearing aids. The researchers' assumption is that mastering the scanpath is essential for achieving optimal results wherever a scanpath representing a tiny solid element consist of only one or a few curves next to one another. While the common materialization route, in which surfaces (like meshes) represent solids starts at the outside (i.e. surface) and moves inward without information as to the engineer's intentions, the researchers' new, alternative approach does not involve such an indirect route and is instead much more direct.

This study also aims to eventually bridge the gap between what is already known and what remains to be discovered, to maximize the potential of PBF-LB/M in case of tiny spatial elements. It is meant to verify the assumption defined by the researchers that control over the exact location of the scanpath enables the engineer to achieve finer details with PBF-LB/M than if the scanpath is generated out of the engineer's sight by a digital system (slicer/hatcher) on the basis of a digital representation of the intended design (in CAD). An additional effect would be that the approach provides the engineer with early insight into the smallest printable feasible with PBF-LB/M.

Dimensions provided in images are in mm

Background

Mastering the scanpath

To materialize a (virtual) geometry by writing lines in successive layers of material, which is called 'scanning', decades ago so-called 'slicing software' and 'hatching software' were introduced with the aim of converting such geometries in a stacking of layers (slices) and to program the toolpath and parameters of the laser (including the scanner) for each layer (hatching, which includes not only hatches). Since the laser is focused in a small spot on the top layer (a few tens of micrometres in diameter), it must move across this powder bed to affect the full cross-section of a parts at the corresponding height. Wherever solids are involved, usually the scanning is accomplished by writing closed contours that represent their surfaces, and hatch patterns within, layer upon layer. Such layers, including (dense) hatches, typically comprise numerous scan lines.

The reason for mentioning this is to highlight a specific aspect of the process: the presence of a very long and winding path that the laser has to travel. In general solids can be handled by engineers easily, but dealing with such a path requires an automated process for slicing and hatching, particularly where high-density hatches are required. In general, the approach is sufficient. There are limitations, however, at the smallest printable sizes, where the dimensions are in the same order as the layer height and the hatch spacing. The engineer must be aware of this in order to deal with them correctly.

Reasons for deviating from the standard route

The default input for most slicers is the .STL file [3], which is a digital representation in the form of a triangulated mesh that approximately describes the surface of a 3D volume modelled in CAD-software.

The slicer output is usually printer-specific or universal but limited to the geometry of each curve in each layer and stored in for instance a Common Layer Interface or .CLI file [4] without information on laser power, scanning speed, etc. Again, having a slicer/hatcher acting as a kind of intermediary between engineering and manufacturing greatly simplifies human effort in the chain of production activities and is therefore important for the industry [5]. But some drawbacks exist, like the one demonstrated below.

Where there is a thin wall, enclosing a narrow area which leaves no room for hatches, the inside offset at one of both long sides may cross the one opposite. Some current slicer/hatchers, such as Renishaw's QuantAM 5, do not include offsets by default in the scan path where they overlap, leaving holes in the print. Such prints are porous or worse. Figure 1 shows an only partially materialized part due to such locally overlapping offsets.

The thickness of the virtual representation of the object is 0.2 mm and the offset to it is 0.1 mm. With a slightly inconsistent distance between the front and back of this 'blade', for example due to the aforementioned .STL inaccuracy, the thickness in some places is just over double the offset, in others less, while the powder bed only is scanned by the laser where the opposite sides are more than 0.2 mm apart.

Figure 1: Variants of a simple thin wall object, printed vertically oriented, with various wall thicknesses (constant for each variant): 0,26 mm on the left and 0,20 mm on the right, showing a poor quality where there are partially overlapping offsets in a 316L PBF-LB/M part (the red curve indicates the height of the section visible in Figure 2, located 12 mm above the build plate).

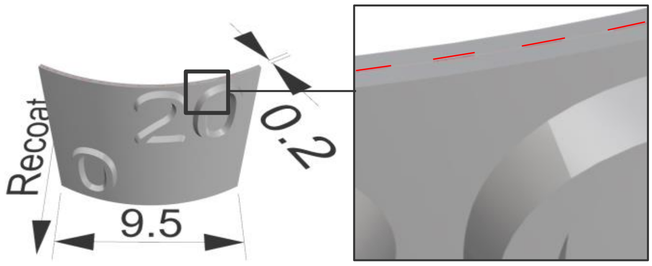

Figure 2: The section of the object visible in Figure 1 in which the location where the laser hits the powder bed is indicated in red, where the offset and the wall thickness do not conflict.

Worth mentioning is that in case the offset of both sides is scanned very close together, but without overlap, the same area is scanned twice. In this study the Renishaw's QuantAM 5 slicer/hatcher was used. The applied RenAM 500S printer setup (by Renishaw, having a 70 µm spotsize) included 316L F (by Carpenter Additive) and a modified parameter set based on Renishaw's default parameter values for running 316L on its 500 series machines (SS316L_500Q_B60_S_01_A.xml of April 2023). The modifications included: layer thickness 30 µm, beam compensation 0.10 mm, border distance 0.05 mm, power 110 W, vertical offset (focus) 0.0 mm, point distance 35 µm, exposure time 30 µs, point delay 0 µs. Figure 2 shows in red the resulting scanpath where the laser hits the powder bed.

Fooling the system to get there

To overcome this behaviour and create the best possible thinnest walls with the highest density and lowest surface roughness, an alternative procedure emerged. It consists of printing an object only represented by a single curve, also known as 'singe-track scanning' [6], or combination of (explicitly specified) curves in each layer instead of a solid. A practical approach was found in the application of non-solids, usually only accepted by slicers/hatchers as support structures. As a work-around to this restriction, non-solid objects (surfaces) were imported in the applied slicer/hatcher as if they were support structures to a (solid) dummy part. For the Renishaw RenAM 500S this meant that 'volume border' values had to be copied to 'support contour' parameters, since a 'volume border' is what remains of a thin wall solid if there isn't enough room for curves inside. These parameters were not expected to be the best possible, but preformed remarkably well and proved very suitable for a proof of concept.

Noteworthy is that it was found that if a (single) curve intended to act as a scanpath is close, some slicers/hatchers, at least Renishaw's QuantAM version 5.3 and GE's Concept Laser WRX Control 2.4, consider the area enclosed by the curve as solid, and by default add an inward offset to compensate for (half of) the thickness the laser will leave behind in the powderbed, while assuming it represents the surface of a solid to be materialized.

Applying a dummy to fool the slicer/hatcher is usually required, while the standard route in AM is (still) largely based on solid models generated virtually in CAD to act as a 'digital twin' (an exact representation in the digital domain of the geometry to be materialized). It's not just Renishaw's software that rejects non-solids acting as parts. In a resent online training of GE related to its M2 Dual Laser Series 5 system (November 2023) there is a tree-like scheme. Where it comes to printing non-solid parts (''CLS Import on the Machine'' > ''Loaded as Part or Support?'' > [''Part''] > ''… Solid or Non-solid?'' > [''Non-solid'']) there is written: ''Adv. Vector Structure (not supported)'', while the voice-over in the video explains: ''Then it would use the advanced vector structure, but again, this is a non-supported behaviour of the machine, because we don't have a supportive tool that would create us those advanced vector structures. … So, in theory, if you would load a non-solid support from Magics [7], 'block support' for example, onto the machine as part, then this would apply. But again, this is non-supported behaviour.'' Such 'advanced vector structures' (a term introduced by Concept Laser, today GE) can be regarded as non-solid objects.

The researchers would like to emphasize here that the use of dummy solids to process non-solids in slicers/hatchers is not entirely unknown. However, an inventory round at some high-tech organizations in Eindhoven (NL), where there are metal printers built by Additive Industries, EOS, Renishaw, SLM Solutions and 3D Systems, learned that most AM experts do not use non-solids except for support structures, and are not aware of such restrictions, let alone how to overcome them.

Two use cases to explain

To investigate on their methodology and to demonstrate the significance, two use cases were introduced: a fountain pen nib and a miniature SMD insulation-displacement connector (IDC).

The fountain pen nib was previously printed in Ti6Al4V ELI based on (the surface of) a solid model, represented by a mesh, processed by a slicer/hatcher. It is intended to be highly customizable, to be produced (i.e. printed) on demand, in small series, without costly tools. With the new methodology it was expected that its minimal thickness could be reduced to achieve better flexibility or 'flex', enabling the user of the nib to create different line widths (due to its non-rigid structure, a flexible nib allows the writer to control the thickness of the line of ink by adjusting the pressure of the pen on the paper). With the new methodology, applied in a hybrid fashion, it was also expected a series of blades inside the monolithic ink buffer or 'feed' in 316L that accompanies the nib, could be printed (Figure 3).

The miniature SMD insulation-displacement connector (IDC) was previously printed in CuNiSi based on (the surface of) a solid model, represented by a mesh, processed by a slicer/hatcher. The concept is intended to be highly customizable with customized parts to be produced (i.e. printed) on demand, in small series without costly tools. With the new methodology, applied in a hybrid fashion, it was expected that the springs and knifes (to cut the insolation) could be improved, for instance to avoid problems like in Figure 1 (Figure 4).

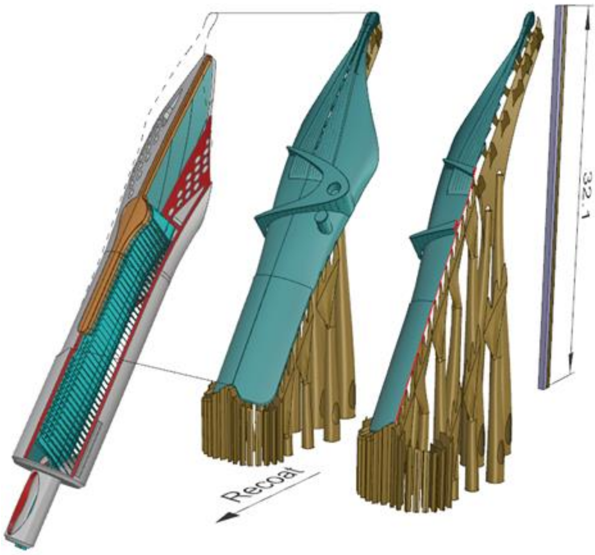

Figure 3: Left - The 'feed', combining solids (light grey), an array of non-solids (turquoise) and a porose (semi-solid) element (orange) | Right - The fountain pen nib (turquoise) and support structures (yellow), both non-solid, with some dummy parts behind.

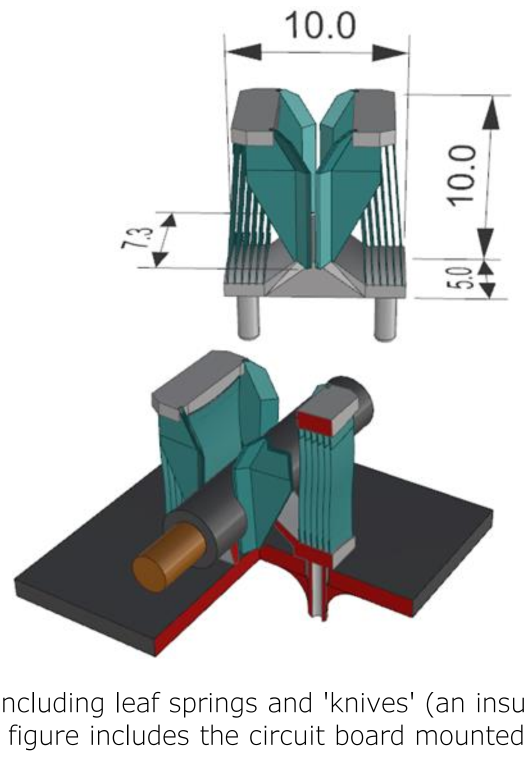

Figure 4: The redesign of an IDC, including leaf springs and 'knives' (an insulation cutting device) as non-solids (turquoise). The lower half of the figure includes the circuit board mounted IDC holding an electric, partially

insulated wire. Because the print also includes conventional solids (light grey), the result is to be classified as 'hybrid'.

Alternative methodology

'Scanpath construction surface'

As mentioned before, manually defining each curve to be scanned is a chore. Therefore an alternative approach was required, but not found, so one was developed. As such, 'scanpath construction surfaces' (SCS) were introduced as surfaces intersecting the layers of the part to be printed, to generate so-called 'scanpath elements', as shown in Figure 5. These intersections are curves by definition. In this concept, such curves are intended to become laser scan vectors where the laser interacts with the powder bed to selectively fuse powder particles together.

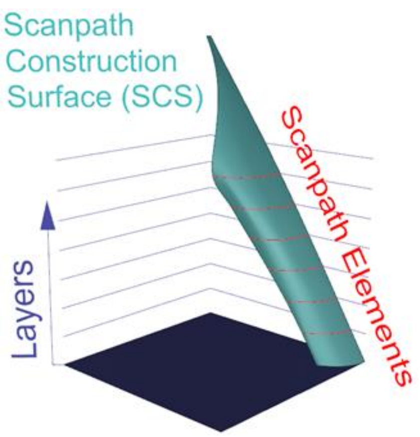

Figure 5: The scanpath construction surface (SCS) applied

That said, one must be aware of the fundamental flaws of this approach. For example, the radius of a fused volume caused by the laser at a single location is related to the spot size, powder, layer thickness, scanning speed and many more parameters. So usually one will have to move the scanpath construction surfaces (manually, if not via a variable in CAD) in order to apply them to a different material or machine, etc. In practice, this may prove a limitation to consider in terms of applicability. However, within this project it was found that when switching from a Renishaw 500S filled with 316L and 30 µm layers to a Concept Laser M2 Dual Laser Series 3 filled with Ti6Al4V ELI and 25 µm layers, it was not necessary to adjust the scan path to secure the usability of the (physical) prints (both use cases).

To at least improve control over the resulting printed geometry, without encountering too much difficulty in defining the exact scan path for the laser to follow, nTopology software, or simply nTop was introduced (nTopology Inc, New York, USA) [8], and two scripts were created. The first, which is the fastest, simply thickens the scanpath construction surfaces. The second however, which is the slowest, first generates curves wherever the scanpath construction surfaces and the layers intersect (i.e. the scanpath) and then thickens these curves. Noteworthy is that all thickening includes the ends of the curves as well as the edges of the surfaces radially.

No significant differences were found between the results generated by both approaches, except for the processing time to get them. It may be appropriate to address this, as thickening these intersections (curves) rather than the scanpath construction surfaces is much more like what actually happens in the printer. However, this absence of differences only exists if the scanpath construction surfaces intersect the layers more or less perpendicularly. If the scanpath construction surfaces (a term coined by the researchers specifically for this) are orientated (nearly) parallel to the layers, the distance in between each curve is too large to result in a single solid (without holes) once combined and thickened. This is demonstrated by Figure 6 and Figure 7, including a solution to this problem in Figure 7. A solution was found in copying the problematic scan path construction surfaces vertically one or more times within the layer height, evenly distributed. And then intersect these extra scanpath construction surfaces with the layers. Here the height of the extra curves might not be perfect, but the layers are usually thin compared to the other dimensions, so the negative effect of this is low.

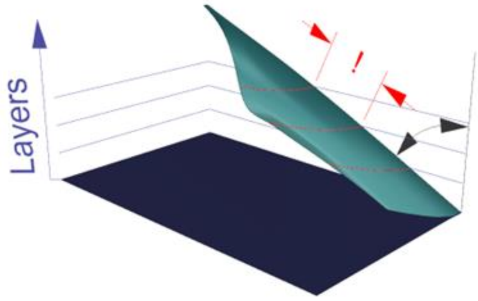

Figure 6: The SCS concept fails where the surface is not (more or less) perpendicular to the layers.

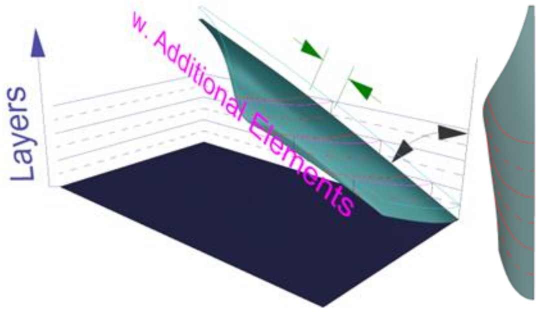

Figure 7: Left - To overcome limitation a copy of the SCS was added and moved vertically | Right - A view from above with the additional scanpath elements included (dashed).

Scripting in nTopology

A limitation of the new method arose from what was described in the previous section: a balanced distribution of path curves for the laser to follow. As previously mentioned, nTopology was introduced, a fairly new software tool with a special focus on 3D printing [8]. With its implicit modelling technology it can handle complex geometries such as for instance dense lattices much faster than conventional tools [9]. With thousands of layers and millions of scan path curve segments, the researchers expected this to be effective.

In nTopology one can write scripts, for example to process 3D data through a series of functions. This can greatly improve the effectiveness of this tool. In this case the key elements in the latest version of these scripts were defined as follows:

a. **Import scanpath construction surfaces** (SCS);
b. **Autogenerate dummy automatically** (for instance by extruding square of 0.5×0.5 mm (in XY; only contour) and a height (in Z) corresponding to height of related non-solid object);
c. **Intersect scanpath construction surfaces and dummy** with all layers;
d. **Create** curves wherever there are such intersections;
e. **Export such curves** to a file the printer (or printer specific slicer) is able to import as slice information (like CLI file; for Concept Laser/GE there is SLC file: one for part [here dummy] and one for support [here non-solid]);

f. **Thicken scanpath construction surfaces** for better understanding of resulting volume in print (fast), visible in Figure 9 (in turquoise

- or -

g. **Thicken curves** to get better understanding of resulting volume in print (slow), visible in Figure 9 (in grey);

h. Optionally: **Export resulting volume as mesh** for communication/iteration in product development, quality control (to compare with high definition 3D scan of materialized result) etc., demonstrated by Figure 8 and Figure 11.

Three other variables were defined and included in the scripts:

a. **Layer Thickness**: the thickness (in Z) of each layer in the print, usually 30 μm (for Renishaw RenAM 500S, at Fontys UAS and ASML Tool Shop) and 25 μm (for Concept Laser M2 Dual Laser Series 3, at FMI Additive);
b. **Single Vector Thickness** (SVT): the thickness of a wall built by a single straight line scanned on each successive layer at the same position (in XY);
c. **Vertically Affected Layers**: the number of layers the laser affects, which is usually more than one.

The single vector thickness is a variable that was created to deal with the volume that a single laser fuses in the powder bed by a single (straight) movement, while considering specific settings for laser power, scan speed, etc. This variable specifically relates to the materialization in XY. Yet in the Z direction, the vertically influenced layer variable relates to the materialization in this direction. In this respect, PBF-LB/M differs from, for example, multi-jet printing solutions, where well defined 'voxels' are produced, like 'pixels' on paper by an inkjet printer [5].

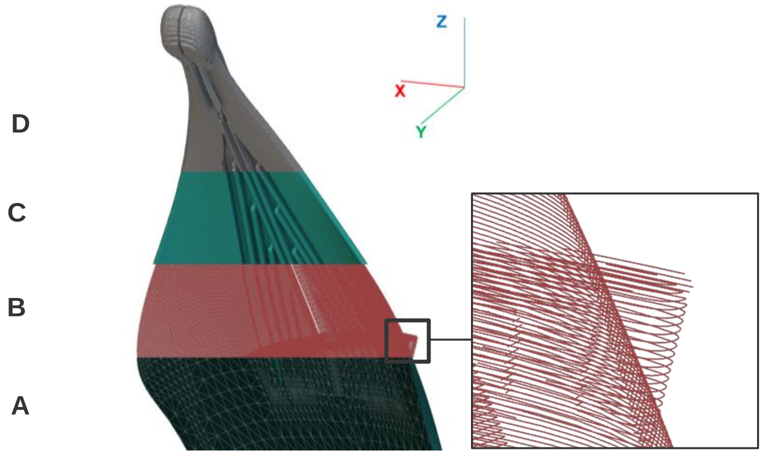

Figure 8: A screenshot of nTopology (4.16.3). A) the scanpath construction surfaces (meshed), B) the intersections surfaces with some layers (result is identical to toolpath), C) the thickened surfaces, D) the mesh created based on thickened surfaces (exported as *.STL).

Key dimensions

PBF-LB/M includes a wide range of key variables that need to be taken into account. An example in case of the Renishaw RenAM 500S with its pulsed-modulated 500W continuous wave ytterbium fiber laser is included in Table 1.

Table 1: Key dimensions applied in the digital twin. 1,2 are fixed, 3-7 applied setting, 8,9 found and applied effects.

	Aspect	Value
a	Material	316L F by Carpenter Additive, non-virgin
b	Spot size	70 µm
c	Vertical offset	0 µm
d	Power	180 W
e	Point distance	35 µm
f	Exposure time	35 µs
g	Layer thickness	30 µm
h	Single vector thickness (XY)	150 µm (in 316L)
i	Vertically affected layers (Z)	5 (considered default)

Here a true voxel would (at least theoretically) measure 150 µm × 150 µm (twice the single vector thickness: along the scanpath as well as perpendicular to it) × 150 µm (5 times the layer thickness). However, as mentioned above, PBF-LB/M in metals differs from multi-jet concepts in that the output of the process is less 'exact', especially in de build direction (Z). Indeed, the powder bed packing density is never 100% and upon solidification the actual printed layer height is therefore smaller than the designed layer height and usually considerably smaller than the spotsize (in XY) [10]. Wherever the laser hits the powder bed, the fusion, given a specific amount of power and exposure time, is highly dependent on the immediate environment of the meltpool. This includes adjacent, previously fused material that acts as a heat sink (much more than what loose powder is capable of, which is related to the density of fused material being almost double) and mirror to the incoming beam [11]. The previously fused material is capable of extracting a significant amount of energy from the meltpool. This can occur via support structures, or through what was previously fused directly below or slightly to the side, in what is known as 'down skin'.

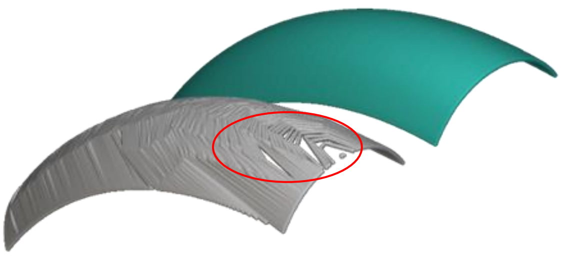

Figure 9: The current results in nTop, with the thickened surface (turquoise) and the thickened curves (grey). The more the surface normal is vertical, the more gaps remain visible between the individual lines (marked by the red ellipse), as addressed in Section 3. The curves are rather angular due to a bug in this not yet officially released nTop 'block' called 'Extract Slice Stack as Graph'.

To gain a better understanding of what affects the quality of non-solid objects, different PBF-LB/M settings were experimented with, assuming that putting a constant amount of energy into this non-solid object would be a practical starting point. Given the pulsed-modulated 500 W ytterbium fibre laser in the Renishaw RenAM 500S, the blade energy density was formulated as follows:

$$Power \times Exposure\ Time \times \frac{1}{Point\ Distance} \times \frac{1}{Layer\ Thickness}$$

Where power is in Watts, exposure time in microseconds, point distance and layer thickness in micrometres, resulting in blade energy density in Joules per square millimetre.

To explain the absence of a volume (but a surface instead), the thickness of such a blade is merely a derivative. It was found that if the power exceeds 200 W, combined with 30 µm layers, stainless steel 316L droplets begin to 'ball' significantly: they merge or fuse in a way that the overall height exceeds the powderbed, preventing the printer's recoater from functioning properly. There was significantly less ball formation after thickening the layers. The effects of adjusted point distance and exposure time were significantly less. It is considered important to conduct further research into this and to explore previously conducted research by others.

These values were applied to the support contour parameters that the printer processes because, as mentioned earlier, the parts were non-solid objects that could only be processed as support structures. In the appendix to this paper some outcomes are listed, including parameter variants for 316L. Several tests were carried out to determine, among other things, the thickness of a non-solid wall perpendicular to XY and at 45 degrees to the platform. The digital 3D models created for this purpose are shown in Figure 10. The smallest distance at which two adjacent leaves are not connected to each other (some 'stickiness' at most) was also examined. In both the experiments in 316L and Ti6Al4V ELI, the blades 0.18 mm and more apart were not connected to each other. Furthermore, it was examined what the minimum distance in the middle of a straight line should be to create two separate blades. Even with the smallest spacing in the digital 3D model, two separate blades were created. In the near future the experiment will be repeated with smaller spacings.

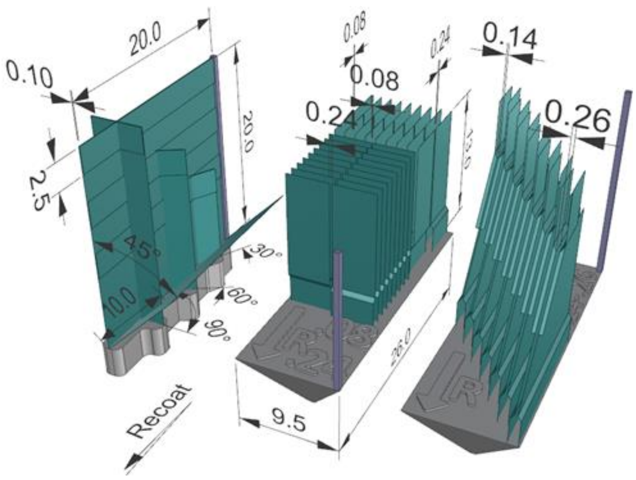

Figure 10: These samples were created by the team to determine some specific properties. Left - Wall thickness | Center - Minimal gap between (stack of) two colinear lines to be apart after materialization | Right - Minimal gap between (stack of) two parallel lines to be apart after materialization.

It was noticed that in the case of Ti6Al4V ELI the spacings are slightly larger than in the supplied file. This experiment will be repeated later, with particular attention to the start and stop delay of the laser of the machine involved: Concept Laser M2 Dual Laser Series 3.

Use case: fountain pen nib

This research effort started after the principal researcher felt uncomfortable about the results he had achieved through the common approach with solid modelling. Particularly where thin elements and high levels of detail were preferred, he found an alternative, more suitable approach by defining the scan path for the laser to follow, rather than relying on software to interpret solid models. The Scanpath Centric Design methodology was introduced. It can be considered a kind of low-level programming language, with very direct input, rather laborious and very strict in its output.

In the figures above, the nib is defined as the small thin part with miniature details, which is ideally suited to show the reader how the new method fits its purpose. The achieved thickness of the central blade is (only) 150-160 µm in 316L and 180 µm in Ti6Al4V ELI. More exciting than the thin blade, is the potential of including tiny additional elements. In this case a space was created right above the feed, including an array of thin walls to secure the ink capacity available to the tip of the nib, since the printed surface is very attractive to fluids like fountain pen ink (Figure 3, Figure 11, Figure 12).

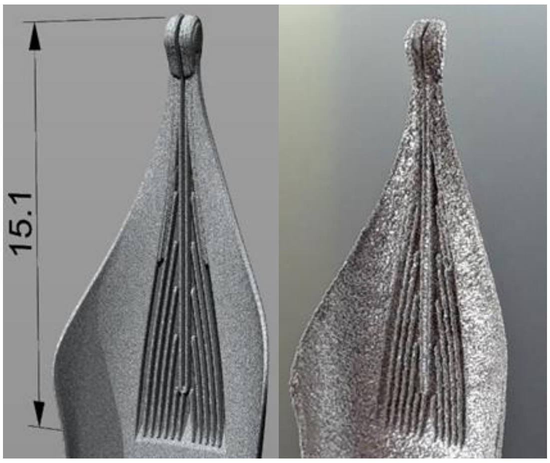

Figure 11: The concave side of the fountain pen nib, including an array of absorptive elements. Left - The mesh output of nTop, rendered in Rhino 5 | Right: The same model, a printed on a Concept Laser M2 Dual Laser Series 3 in Ti6Al4V ELI having 25 µm layers.

The solid elements involved (both the tip of the nib and the logo) were created in the same way, including a pattern to fill these (small) volumes. Because the team was unsure about the exact start and stop position of the Concept Laser M2 Dual Laser Series 3 lasers without activating an option to make the laser move between the scan path elements in a smooth motion, called 'skywriting', some planes perpendicular to one another were adjusted in CAD, so that their interconnection became parallel, significantly reducing the impact of this. Later on this was also applied to the edges along the split of the nib. Not only did it secure the width of the slit, it also appeared to increase the usability of the nib while it is used for writing (Figure 13).

Figure 12: One of the first prints based on the 'non-solid' version of the 3D printed fountain pen nib, printed in Ti6Al4V ELI. Below the nib is the 'feed', printed in 316L. Due to the small thickness, the nip has quite a bit of 'flex'. The assembly functions well. However, the surface finish of the nib is expected to have room for improvement.

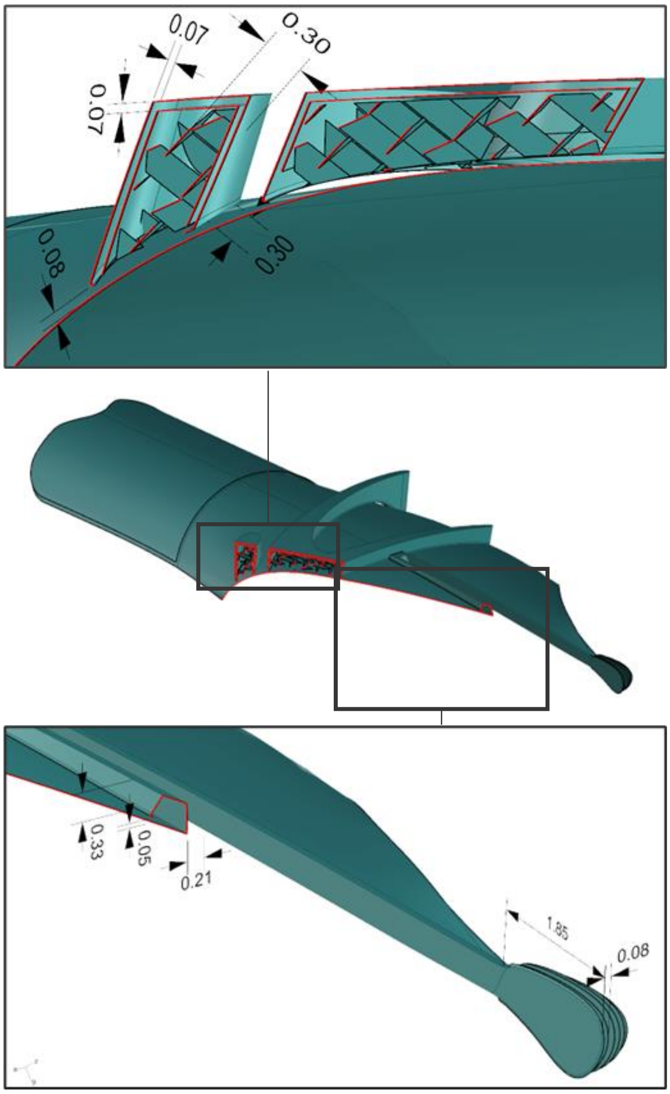

Figure 13: The fairly 'solid' elements in the fountain pen nib, including the logo, the tip and the raised edges along the slit, with the scanpath generated by applying the SCD concept. In the CAD model, the logo is not attached to the blade, with a small space of 0.08 mm in between to limit the effects of the formation of the logo on its convex side.

The reader may like to know that on the concave side of the printed nib, ink absorption is useful and common behaviour for such a printed surface, while on the convex side, to prevent this, a nano coating has been effectively applied [12].

Use case: miniature SMD insulation-displacement connector

Based on a design created in 2017, a printable miniature surface-mounted (SMD) isolation-displacement connector (IDC, to be printed in CuNiSi) was recreated with the Scanpath Centric Design applied on some of the functional elements: leaf springs and 'knives'. For reader's understanding, the component allows an installer to connect an insulated electrical wire to a printed circuit board (PCB) in a single (manual) action. The leaf springs and knife-like elements to cut the insulation while the electrical wire is pushed into the connector, electrically connected and held in place, were included in the digital model as scanpath construction surfaces. Only where some added value of the Scanpath Centric Design methodology was expected was it applied, while elsewhere solids were applied. So the result is to be classified as 'hybrid'. Despite the lack of the right material (CuNiSi), the interim results (Ti6Al4V ELI) largely demonstrate the added value of applying scanpath construction surfaces. It is concluded that it is very applicable (Figure 4, Figure 14).

Figure 14: The IDC, in the absence of CuNiSi, printed in Ti6Al4V ELI on a Concept Laser M2 Dual Laser Series 3 having 25 µm layers. The result suggests an effective application of the Scanpath Centric Design method once printed in the intended copper alloy.

Conclusions and outlook

In metal powderbed fusion with laser (PBF-LB/M) more direct control over the scan path can offer added value if the elements to be printed are very small, with sizes close to the spotsize and hatch spacing applied. Manually or semi-manually defining the shape and position of this path by the engineer is very laborious. A method was developed to mitigate that and to generate a digital twin to verify the result once materialized, as most currently available software does not widely support control over individual scan path curves. It was named Scanpath Centric Design (SCD).

It was found that the new methodology has nothing to offer in case of more voluminous parts. However, it was also found that the traditional approach via solid models can be easily combined with SCD in a hybrid fashion. It allows the engineer to effectively construct the smallest possible design features in PBF-LB/M, and offers a feedback loop to evaluate how the 'designed' scanpath will materialize.

This publication is intended to introduce a new methodology, one that spans multiple succeeding steps in the value chain, and should stimulate further research, more quantitative than qualitative. It was noted that where a stack of scan path curves is the smallest element available to the engineer, much remains to be explored. It is expected that much is be derived from adjacent research regarding thin wall fabrication in AM [13] [14] [15] [16] and microscale laser powder bed Fusion [6] (and many more publications). Further research will focus on the thinnest possible elements in different combinations and orientations (Figure 15), which may include curve and pulse segmented as well as multiple scanning.

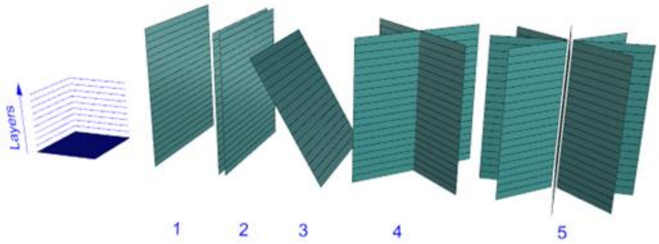

Figure 15: Some basic shapes with the thickness of a single laser pass ('single track') or just a few of them to be examined and optimized, also in interaction with each other, with emphasis on surface quality and density:

1. A vertically constructed wall;
2. A few walls built right next to each other;
3. A wall that is not constructed in the build direction;
4. Multiple intersecting walls (not necessarily intersecting perpendicularly);
5. A local accumulation of fusions (and thus energy accumulations).

These also in combination with each other.

One of the future use cases is this design of a flexure pivot below with intersecting blades (Figure 16). Again hybrid, so a combination of the standard methodology that includes solids and some scanpath construction surfaces (SCS) to have better control over how the leaf springs get scanned layer by layer. The result will be tested for accuracy and durability. The outer diameter is 40 mm and the thickness of (most of) the leaf springs (once printed) 0.3 mm.

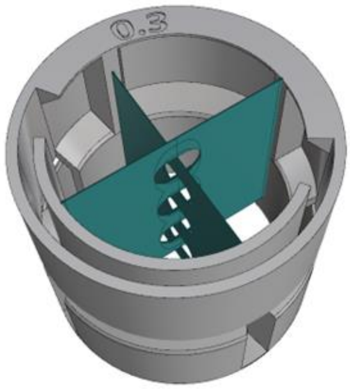

Figure 16: Flexure pivot design having SCD applied on the leaf springs (turquoise) [17]

Contact details

Rein van der Mast (Corresponding author)

E-Mail: r.vandermast@fontys.nl

E JOURNAL

References

[1] Wohlers, T., Wohlers Report 2022: 3D Printing and Additive Manufacturing Global State of the Industry, Wohlers Associates, 2022.

[2] N. Y. C. P. S. R. S. D. L. R. G. D. B. Sohini Chowdhury, „Laser powder bed fusion: a state-of-the-art review of the technology, materials, properties & defects, and numerical modelling," *Journal of Materials Research and Technology,* Bd. 20, Nr. September–October 2022, pp. 2109-2172, 2022.

[3] P. K. R. K. M. H. S. Ajay Kumar, "Printing file formats for additive manufacturing technologies," in *Advances in Additive Manufacturing / Artificial Intelligence, Nature-Inspired, and Biomanufacturing*, vol. Additive Manufacturing Materials and Technologies, Elsevier, 2023, pp. 87-102.

[4] J. P. J. Ö. Anton Wiberg, „Design for additive manufacturing – a review of available design methods and software," *Rapid Prototyping Journal,* Bd. 25, Nr. 6, pp. 1080-1094, 6 August 2019.

[5] D. R. ,. B. S. ,. M. K. Ian Gibson, Additive Manufacturing Technologies, Springer Cham, 2021, p. 675.

[6] Z. Xiong, L. Haohang, H. Yang, Y. Yang, L. Yinong, L. Cui, X. Li, L. Masseling, L. Shen und S. Hao, „Micro laser powder bed fusion of NiTi alloys with superior mechanical property and shape recovery function," *Additive Manufacturing,* Bd. 57, Nr. 102960, p. 12, 2022.

[7] Materialise, „Materialise Magics," Materialise, [Online]. Available: https://www.materialise.com/en/industrial/software/magics-data-build-preparation.

[8] nTopology, „nTopology," [Online]. Available: https://www.ntop.com/.

[9] Y. F. Z. Nikita Letov, "A geometric modelling framework to support the design of heterogeneous lattice structures with non-linearly varying geometry," *Journal of Computanional Design and Engineering,* vol. 9, no. 5, p. 1565–1584, October 2022.

[10] G. L. F. K. T. C. Jean-Pierre Kruth, „Consolidation phenomena in laser and powder-bed based layered manufacturing," *CIRP Annals,* Bd. 56, Nr. 2, pp. 730-759, 2007.

[11] L. T. B. V. H. Umberto Paggi, „Implementation of contactless supports for industrially relevant additively manufactured parts in metal," *Additive Manufacturing Letters,* p. 100095, 2022.

[12] L. Kan, L. Zhang, P. Wang, Q. Liu, J. Wang, B. Su, B. Song und Y. Shi, „Robust Superhydrophobicity through Surface Defects from Laser Powder Bed Fusion Additive Manufacturing," *Biomimetics,* Bd. 8, p. 598, 2023.

[13] Z. Wu, S. Prabha Narra und A. Rollett, „Exploring the fabrication limits of thin-wall structures in a laser powder bed fusion process," *The International Journal of Advanced Manufacturing Technology* , Bd. 110, p. 191–207, 11 August 2020.

[14] H. Jia, H. Sun, H. Wang, Y. Wu und H. Wang, „Scanning strategy in selective laser melting (SLM): a review," *The International Journal of Advanced Manufacturing Technology,* Bd. 113, p. 2413–2435, 24 February 2012.

[15] T. Larimian, B. AlMangour, D. Grzesiak, G. Walunj und B. Tushar, „Effect of Laser Spot Size, Scanning Strategy, Scanning Speed, and Laser Power on Microstructure and Mechanical Behavior of 316L Stainless Steel Fabricated via Selective Laser Melting," *Journal of Materials Engineering and Performance,* Bd. 31, p. 2205–2224, 14 November 2021.

[16] E. Malekipour und H. El-Mounayri, „Scanning Strategies in the PBF Process: A Critical Review," in *Proceedings of the ASME 2020 International Mechanical Engineering Congress and Exposition*, Virtual, Online, 2021.

[17] J. H. J. Janssen und R. H. A. v. Lieshout, „Robot joint as well as robot arm provided with such robot joint". WO Patent WO2020159365A1, 2019.

[18] R. v. d. Mast, „3d print of the nib of a fountain pen (pending)". EU Patent EP3323627A1, 2016.

[19] Z. Wu, S. Prabha und A. Rollett , „Exploring the fabrication limits of thin-wall structures in a laser powder bed fusion process," *The International Journal of Advanced Manufacturing Technology,* Bd. 110, p. 191–207, 11 August 2020.

[20] T. T. Wohlers, I. a. Campbell, O. a. Diegel, R. a. Huff, J. a. Kowen and W. A. (Firm), "Wohlers report 2022 : 3D printing and additive manufacturing global state of the industry," Wohlers Associates, 2022.

[21] A. P. J. Ö. J. Wiberg, "Design for additive manufacturing–a review of available design methods and software," *Rapid Prototyping Journal,* vol. 25, no. 6, pp. 1080-1094, 2019.

[22] W. UAS. [Online]. Available: https://3diamm.nl.

Acknowledgements

The authors express their sincere thanks to the Catholic University of Leuven – Additive Manufacturing Research Group (Leuven, Belgium), Fontys University of Applied Sciences – Engineering (Eindhoven, Netherlands), ASML (Veldhoven, Netherlands), FMI Additive (Tilburg, Netherlands), FMI Instrumed (Schiedam, Netherlands) and Materialise (Leuven, Belgium).

The use cases were based on creations of the principal researcher and initiator, Mr. Van der Mast, including the world's first 3D printed metal fountain pen nib [18] and feed, as well as the printable IDC he created in 2017 for a multinational company that produces connectors, sensors, relays, contactors and application tooling for several industries.

Declarations

Code availability The nTop scripts are available upon request from the corresponding author.

Appendix

Figure 17: Variants explored to find effects of different parameters on blade generation

Alt name	Runs (test No)	Layer Thickness (µm)	Power (W)	PointDistance (µm)	ExposureTime (µs)	Energy (J/mm²)	Build canceld at parts' layer	Result score[1]	Thickness[2] blade 90° to XY (mm)	Thickness[2] blade 45° to XY (mm)	Perf.[3] in blades near intersections	Perf.[3] In blade 45° to XY
		<SUPPORT CONTOUR>										
C9_Alt-S4-019	4	30	180	15	20	8,00	-	3	0.13	0.17		X
C9_Alt-S4-007	2,3	30	180	35	35	6,00	-	2,3,4	0.15	0.17	X	
C9_Alt-S4-002	2,3,4,5	30	120	13	20	6,15	-	3	0.13	0.17		X
C9_Alt-S4-003	2,3,4,5	30	120	20	30	6,00	-	3	0.13	0.16		
C9_Alt-S4-005	2,3,4,5	30	160	13	20	8,21	-	3	0.14	0.16	X	
C9_Alt-S4-008	2,3,4	30	120	35	70	8,00	-	3,4	0.14	0.16		
C9_Alt-S4-004	2,3	30	**240**	20	20	8,00	50	1,4				
C9_Alt-S4-016	4	30	**200**	50	60	8,00	41	1				
C9_Alt-S4-011	2,3	30	**270**	45	30	6,00	36	1				
C9_Alt-S4-009	2,3	30	**315**	35	20	6,00	33	1				
C9_Alt-S4-013	2,3	30	**200**	20	30	**10,00**	33	1				
C9_Alt-S4-017	4	30	**200**	40	60	**10,00**	27	1				
C9_Alt-S4-022	4	30	180	20	34	**10,20**	17	1				
C9_Alt-S4-014	2,3	30	**200**	35	53	**10,10**	12	1				
C9_Alt-S4-012	2	30	**360**	45	30	8,00	10	1				
C9_Alt-S4-006	2,3,4	30	160	20	30	8,00	421	1,4				
C9_Alt-S4-001	2,3,4,5	30	180	20	20	6,00	408	1	0.13	0.17	X	X
C9_Alt-S4-020	4	30	120	20	50	**10,00**	288	1				
C9_Alt-S4-015	4	30	180	50	67	8,04	173	1				
C9_Alt-S4-021	4	30	160	20	38	**10,13**	167	1				
C9_Alt-S4-010	2	30	**420**	35	20	8,00	100	1				
~~C9_Alt-S4-018~~	~~4~~	~~30~~	~~**220**~~	~~55~~	~~60~~	~~8,00~~	-					
C9_Alt-S4-023	5[4]	30	135	20	20	4,50	-	-3				

Remark	Result score	Explanation
1	1	Build aborted, above powderbed and danger to recoater
	2	Scan clearly visible after recoat, no danger to recoater
	3	Clear run
	4	Patterns visible in surface
2	Measured without post-processing, performed indicatively. Within the same sample and between identical samples within the same build and different builds, differences of up to +/- 0.02 mm were found. It has therefore been decided to investigate this further at a later date. Also, it is now hypothesized that in this configuration, blades that are not vertically oriented are thicker, about 0.02 to 0.03 mm if at 45° to the platform.	
3	When held up to a bright LED light source, some samples appeared to have holes at the intersections between both (vertical) blades, others had in the blade at 45° to the platform, and some both. It has therefore been decided to investigate this further at a later date.	
4	Not tested, but successfully applied on fountain pen nib and insulation-displacement connector	

1st Printer	Renishaw RenAM 500S (70 µm spotsize)
Material	316L (ASTM F3184) Carpenter Additive F variant, non-virgin
Atmosphere	Argon 5.0
Platform temp	170 °C
Layer thickness	30 µm
Focus	No vertical offset

2nd Printer	Concept Laser M2 Dual Laser Series 3 (50 µm spotsize)
Slicer/Hatcher	Materialise Magics Concept Laser Slicer / Concept Laser WRX Control 2.4
Material	Ti6Al4V ELI (ASTM F3001) non-virgin
Atmosphere	Argon 5.0
Platform temp	Room temperature

Layer thickness	25 µm
Focus	- 0.4 mm
Power	110 W
Laser speed	900 mm/s[+]

[+]) Both lasers of the dual laser system were applied, but only one laser per part. No significant differences were found.